J Appl Electrochem (2007) 37:737–746
DOI 10.1007/s10800-007-9306-4

ORIGINAL PAPER

Electrochemical impedance and conductivity measurements in a heterogeneous Fe powder particle—electrolyte system with or without electrochemical reaction

M. F. Gál · J. Híveš · M. Benová · M. Gálová

Received: 8 December 2004 / Accepted: 31 January 2007 / Published online: 7 March 2007

Abstract The participation of solid Fe powder particles in the transfer of charge through a heterogeneous system consisting of an electrolyte and conducting powder particles was studied by means of electrochemical impedance spectroscopy and conductivity measurements. Different behaviour was encountered in electroinactive Na_2SO_4 electrolyte without metal electrodeposition on the Fe particles and in $NiSO_4$ electrolyte where Ni electrodeposition occurs on the Fe particle surfaces. From impedance diagrams and the proposed model the formation of aggregates and chains of Fe particles is deduced. The important role of electrochemical reaction proceeding at the particle surface in the charge transfer behaviour in stirred heterogeneous systems was also demonstrated.

Keywords Electrochemical deposition · Electrochemical impedance spectroscopy · Fe powder · Ni coating · Transfer of charge

M. F. Gál
J. Heyrovského Institute of Physical Chemistry,
The Academy of Sciences of the Czech Republic,
Dolejškova 3, 182 23 Prague, Czech Republic

J. Híveš (✉) · M. Benová
Faculty of Chemical and Food Technology, STU,
Radlinského 9, 812 37 Bratislava, Slovakia
e-mail: jan.hives@stuba.sk

M. Gálová
Institute of Chemistry, P.J. Šafárik University, Moyzesova
11, 04001 Kosice, Slovakia

1 Introduction

Several authors have dealt with charge transfer behaviour in fluidized bed electrodes [1–7]. However, few papers describe the charge transfer mechanism in stirred heterogeneous systems [8, 9].

In our laboratory, research has been carried out on the electrochemical coating of powder materials [8–11]. The transfer of charge is one of the factors affecting electrodeposition processes in stirred heterogeneous systems.

The mechanism of charge transfer through a heterogeneous system may differ even for the same system depending on the conditions. The following mechanisms have been suggested for fluidized bed electrodes: simple ionic conductance, short circuit conductance, collision [2] and a ''conducting'' mechanism [3]. Simple ionic conductance occurs due to ions. Short circuit conductance means that the charge passes through the solid particle by an electronic mechanism in addition to ionic conductance. The collision mechanism [2] assumes that in the heterogeneous suspension the charge is transported by collisions of particles both with each other and the current feeder. The ''conducting'' mechanism supposes charge transfer through short-lived chains or aggregates of particles. Disintegration and new formation of the chains and the aggregates cause current fluctuations and local overvoltage in the bed. Thus the participation of solid metallic particles in the charge transfer process should be considered. One can also expect these mechanisms to affect charge transfer in stirred heterogeneous systems. Initial results obtained in this field have been published [9].

Analysis of experimental results obtained from EIS and conductance measurements and a simplified model

of a heterogeneous system will be presented in this paper. Due to the low frequency of contact of powder particles [12] with the current feeder, N_{con}, the model designed for a similar system by Galova et al. [8] could not be used. The conclusion was made that not only particles in contact with current feeder, but also particles in the bulk of the electrolyte are able to carry the charge. Chains or aggregates of particles formed in the system are responsible for the charge transfer.

Charge transfer in such a system may be realized by both solid and solution phases depending on their respective conductivity. The conductivity of the system is influenced negatively by the insulating particles, while conducting ones contribute to the overall conductivity of the heterogeneous system [1, 9]. In the latter case, the contribution depends on both concentration and particle size. Both effects are represented by the so called voidage factor ε defined as [13]

$$\varepsilon = \frac{V_e}{V_e + V_p} \quad (1)$$

V_e is the electrolyte volume and V_p the particle phase volume. For stirred systems the density of the suspension of solid particles in the electrolyte is expressed as (1–ε).

2 Experimental

Iron powder was sieved into four granulometric fractions: 45–63, 63–100, 100–125, 125–160 μm. Prior to electrolysis, the powder was activated chemically by reduction in a 10 wt% hydrazine hydrochloride solution for 3–5 min followed by distilled water and acetone wash, then dried.

A 0.6 M Na_2SO_4 (pH = 5.6) as electroinactive electrolyte (no metal electrodeposition on Fe particles at applied potential) and a 0.6 M $NiSO_4$ (pH = 4.5) as electroactive electrolyte (electrochemical deposition of Ni at the powder surface) were utilized. The powder was kept in suspension by a mechanical stirrer set to 210 rpm.

An acrylic glass cell designed in our laboratory and shown in Fig. 1 was used for both impedance and conductance measurements. Both cathode and anode were graphite. The cathode surface area was 4 mm^2 and the anode was 400 mm^2. As shown in Fig. 1, the transfer of powder particles from cathodic into anodic compartment was prevented by the cell construction. Replacement of the reference electrode by a conductance electrode was made during conductance measurements.

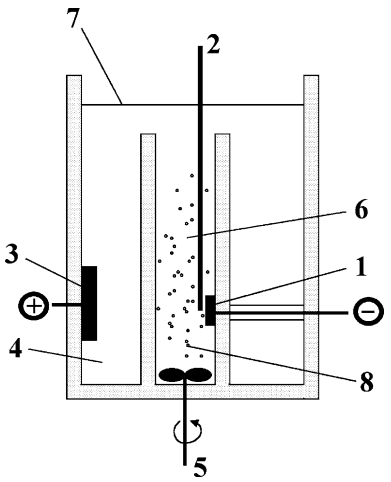

Fig. 1 Scheme of the measuring cell. 1—working electrode, 2—reference electrode, 3—counter electrode, 4—anodic compartment, 5—mechanical stirrer, 6—cathodic compartment, 7—electrolyte level, 8—powder particles

Impedance measurements were recorded using a laboratory-built electrochemical system [14] consisting of a fast rise-time potentiostat interfaced to a personal computer via the IEEE-interface card PcLab model 748 (AdvanTech Co., USA). Voltage sources were either a 12-bit D/A card PcLab model 818 or a programmable arbitrary-function generator Stanford Research model DS340. The impedance measurements were carried out in the range 1 Hz–100 kHz using a network analyzer (Stanford Research model SR780).

The *ac* amplitude of 10 mV was derived from an internal oscillator of the network analyzer. A three-electrode electrochemical system was used with an Ag/AgCl in 1 M—LiCl reference electrode separated from the test solution by a salt bridge. DC polarization of—600 mV versus reference electrode was used in both Na_2SO_4 and $NiSO_4$ electrolytes. Each impedance curve consisted of 100 measured points. The conductance measurements were carried out using a conductometer K912 (Consort) equipped with a four-electrode flow system S612T (Consort) especially designed for the experiments in suspensions.

3 Results and discussion

3.1 Na_2SO_4 electrolyte

As mentioned previously, no metal electrodeposition at the iron particle surface is possible in Na_2SO_4 electrolyte at—600 mV. The reduction of dissolved oxygen in the solution is probably the only process that occurs.

The data shown in Fig. 2 demonstrate the influence of powder particles on the shape of the impedance measurement. A new loop is visible in the high-frequency region upon addition of powder. This feature cannot be ascribed to the influence of the electrolyte. The new loop appears to be closely connected with the presence of dispersed powder particles fluidized in the electrolyte colliding with the current feeder and, even more frequently, against each other. As shown in Fig. 3 the conductance of the suspension formed by electrochemically non-active electrolyte Na_2SO_4 and Fe powder decreases with increasing suspension density in all granulometric fractions studied. Conductance increases with increasing particle size. This is due to the significant reduction in the number of particles in the electrolyte. At constant suspension density the ratio of the smallest particles to the largest is 18:1. A possible interpretation of this effect is that ionic conductance is hindered by the high number of particles in a non-active electrolyte. At high suspension densities a limitation in the conductivity of all particle size fractions is observed. This is due to the change in the role of iron particles in the electrolyte. At high suspension densities they not only hinder ionic conductance but contribute to charge transfer by mutual collisions and formation of aggregates. This effect becomes more dominant as the suspension density increases. If the powder particles are non-conducting, e.g. Al_2O_3, they act exclusively to lower the ionic conductance and the higher their concentration the greater this reduction [9].

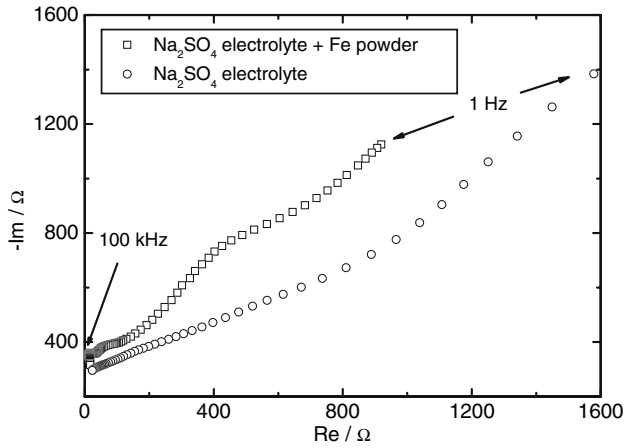

Fig. 2 Electrochemical impedance spectra of: ○—0.6mol dm^{-3} Na_2SO_4 electrolyte (basic electrolyte); □—basic electrolyte + iron powder (4 g) of the size fraction 100–125 μm

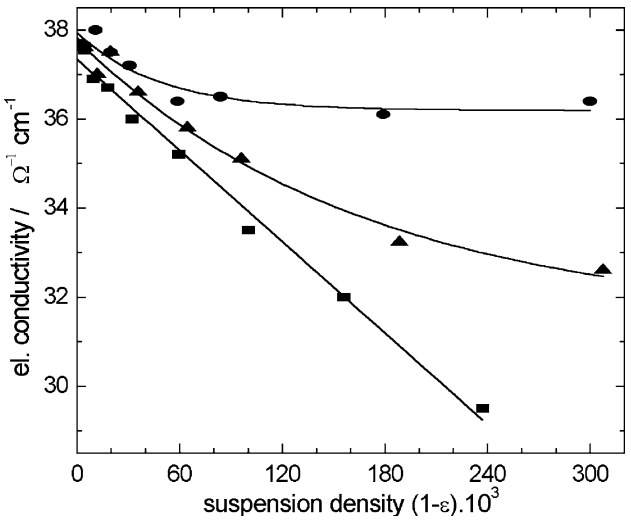

Fig. 3 Electrical conductivity of suspension versus density of suspension in a system consisting of Na_2SO_4 electrolyte and iron powder for various size fractions of the iron powder: ● 125–160 μm; ▲ 100–125 μm;■ 45–63 μm

3.2 *$NiSO_4$* electrolyte

Ni electrodeposition on the iron powder particles and graphite cathode occurs in $NiSO_4$electrolyte. The overall electrode reaction proceeding on the graphite cathode can be summarized as $Ni^{2+} + 2e^- = Ni$. After the immersion of Fe powder into $NiSO_4$ electrolyte an immediate exchange reaction $Fe+Ni^{2+} = Fe^{2+} + Ni$ also proceeds.

The differing behaviour of the two heterogeneous systems, $NiSO_4$(el)–Fe(pp) and Na_2SO_4(el)–Fe(pp), is presented in the impedance plot in Fig. 4. Only one loop corresponding to Ni deposition on the compact cathode is observed without powder particles. Upon addition of the powder a new loop in the high-frequency region followed by another one corresponding to Ni electrodeposition is observed.

By comparison with literature data [7] the influence of the suspension density on the shape of the impedance

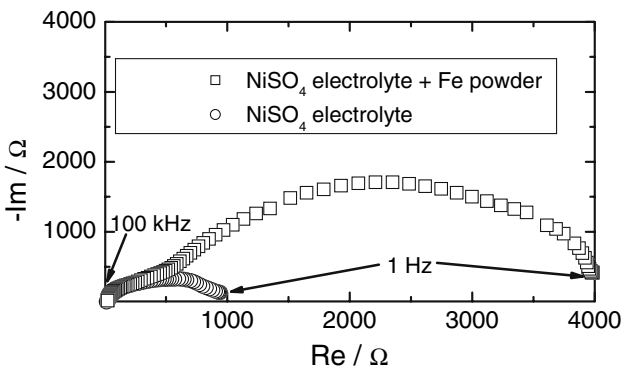

Fig. 4 Electrochemical impedance spectra of: ○—0.6mol dm^{-3} $NiSO_4$ (basic electrolyte); □—basic electrolyte + iron powder (10.5 g, $1-\varepsilon = 163.3 \times 10^{-3}$) of the size fraction 100–125 μm

spectrum in Fig. 5 shows no gradual disappearance of the first high-frequency loop. Only a remarkable reduction of the loop attributed to the deposition of Ni on the compact electrode is apparent in Fig. 4. The difference may be attributed to the fact that in the electrolyte used by Gabrielli [7], the number of particles stays the same, while the change of the flow-rate causes the variation in the suspension density. At zero flow-rate, the particles behave as a packed bed electrode where their mutual contact is permanent and not intermittent as in a fluidized bed. Thus no loop is observed in the high-frequency region. A loop in the high-frequency region attributed to the collisions of the powder particles appears when the flow-rate of the electrolyte minimally increases.

Gradual reduction of the loop in the low-frequency region may be explained by the increasing surface area of the electrode due to the engagement of the powder particles in the electrochemical process of Ni deposition. The different composition of the current feeder and powder particles is the cause of the different impedance diagrams recorded on the current feeder and powder particles. Similar results were observed earlier using a copper electrode [9].

The conductivity of the system $NiSO_4$–Fe powder shows fluctuations in time in contrast to the system Na_2SO_4–Fe powder. A general increase in electrical conductivity is observed (Fig. 6). This corresponds to the statement that conducting powder particles contribute to charge transfer more in stirred systems with an electrode reaction proceeding at their surface than in systems without stirring. Such fluctuations, caused by random collisions of particles and collisions with the current feeder, were observed in our earlier work and other previous cases [7, 9]. Stable aggregates of particles sticking to each other by the deposited Ni layer may be formed. A similar appearance of Fe particles

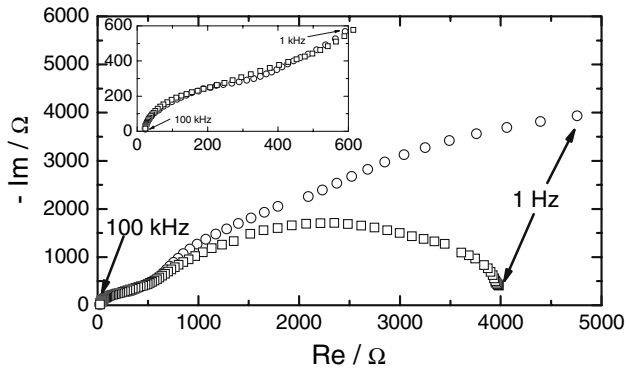

Fig. 5 EIS spectra of 0.6 mol dm^{-3} $NiSO_4$ electrolyte: ○—2g of the iron powder ($1–\varepsilon = 14.7 \times 10^{-3}$); □—10.5 g of Iron powder ($1–\varepsilon = 163.3 \times 10^{-3}$) of the size fraction 100–125 μm

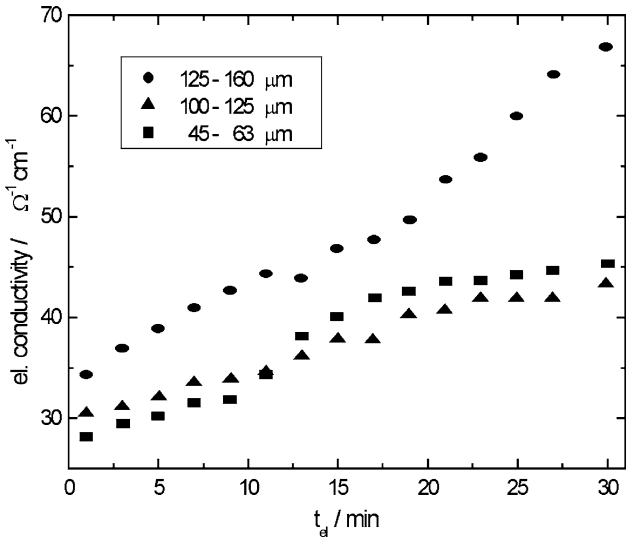

Fig. 6 Change of the suspension electric conductivity with electrolysis time for various size fractions of the iron powder: ● 125–160 μm; ▲ 100–125 μm; ■ 45–63 μm; suspension density: $1–\varepsilon = 53.5 \times 10^{-3}$; electrolyte: 0.6 mol dm^{-3} $NiSO_4$

stuck by deposited Ni layer on the current feeder surface after 30 min of constant current electrolysis in $NiSO_4$ solution is observed.

In the system with increasing particle concentration (Fig. 7) the probability of chains and aggregate formation increases. A gradual change from the simple ionic conductivity in the system without solid particles to the ''conducting'' mechanism in the system with iron particles has occurred. The significance of the

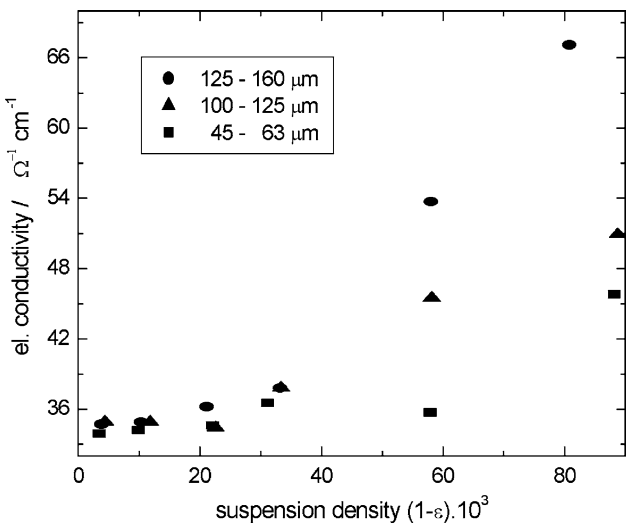

Fig. 7 Electrical conductivity of suspension versus density of suspension in a system consisting of $NiSO_4$ electrolyte and iron powder for various fraction size of the powder: ● 125–160 μm; ▲ 100–125 μ m; ■ 45–63 μm

electrochemical reaction proceeding in the system at the particle surface is evidenced by comparing the data shown in Fig. 7 with that in Fig. 3. From Fig. 7 it may also be concluded that the number of actually charged Fe particles is not proportional to the number of gradually added particles. Only a fraction of the particles becomes charged as a consequence of collision with other particles or the current feeder. Other uncharged particles represent a natural obstacle to transportation of ions carrying charge and thus, to ionic conductance. The number of charged particles increases and, consequently, the character of the conductivity of the suspension changes with time (Fig. 6).

The electrochemical behaviour of the heterogeneous system was represented by EIS as an equivalent circuit. For the evaluation of the equivalent circuit parameters from experimentally recorded complex impedances, direct calculation from the equivalent circuits and AUTOLAB software developed by ECOchemie (Holland) were used.

Following the work of Gabrielli et al. [7] we used a transmission line to interpret experimentally obtained impedance spectra. The general scheme is shown in Fig. 8.

For Ni electrolyte the particular impedances Z_m and Z of the transmission line are given in Figs. 9 and 10, respectively.

The calculation and digital simulation show that the appearance of a capacitive loop in the high frequency region is related to the circuit (R_{con}, C_{con}) and in the low frequency region is related to the circuit (C_{dl}, [R_{ct}, O]). Therefore, the contact impedance Z_m shows a capacitive feature. Without capacity C_{con}, the loop does not appear in the high frequency region. This contact impedance is related to a time average value taken over all mutual intermittent contacts among individual particles and particles with the current feeder.

The digital simulation of impedance data also shows that the "O" diffusion element must be implemented into interfacial impedance Z instead of the more often used Warburg impedance, dealing with the semiinfinite thickness of the diffusion layer. In stirred heterogeneous systems there is a region close to the electrode in which the mass transport occurs only by diffusion. Outside of this so-called Nernst Diffusion Layer (NDL) the solution is homogeneous due to stirring. The concentration of the diffusing species in the bulk solution remains unchanged. The material simply diffuses through the NDL to reach the electrode. The impedance in this case is described by the so-called "O" circuit element. It can be expressed as:

$$\mathrm{Z} = \frac{1}{Y_0\sqrt{i\omega}}\tanh(\mathrm{B}\sqrt{i\omega}) \tag{2}$$

where Y_0 is the magnitude of the admittance (= 1/Z) at ω = 1 rad/s(~0.16 Hz). If the thickness of the NDL is δ, then the constant B is related to that thickness and the diffusion coefficient D. Therefore, B characterizes the time it takes for a reactant to diffuse through the NDL.

$$\mathrm{B} = \frac{\delta}{\mathrm{D}^{1/2}} \tag{3}$$

In heterogeneous stirred systems an accurate quantification of the diffusion coefficient is not simple. The electrochemical response is not controlled purely by diffusion due to the intermittent contacts and turbulent movement of particles. The mass transport involves a substantial contribution from convective transport. Therefore, the diffusion coefficient was kept constant for all calculations ($\mathrm{D} = 1 \times 10^{-5}\mathrm{cm}^2\ \mathrm{s}^{-1}$).

In Fig. 11 the results of non-linear regression analysis are presented. Satisfactory agreement between the experimental results and non-linear regression analysis calculations can be observed.

The total impedance of the system according to equivalent circuits (Figs. 9, 10) can be expressed as

$$Z_T = i\omega L_{out} + R_{el} + \frac{R_{con}}{i\omega C_{con}R_{con} + 1} + \\ + \frac{i\left(R_{ct} + Y_0\sqrt{i\omega} + \tanh\left(B\sqrt{i\omega}\right)\right)}{iY_0\sqrt{i\omega} - R_{ct}C_{dl}Y_0\omega\sqrt{i\omega} - \omega C_{dl}\tanh\left(B\sqrt{i\omega}\right)} \tag{4}$$

The first term in this equation, L_{out}, is constant for all particle sizes and is also independent of the number of

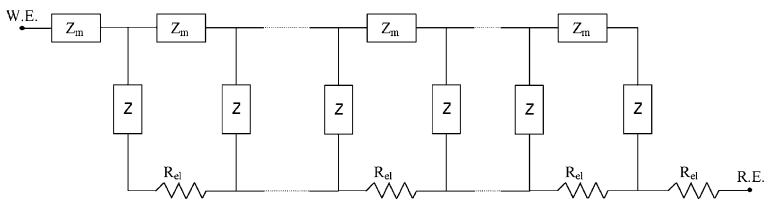

Fig. 8 General scheme of the transmission line used as a model of heterogeneous system for electroactive electrolyte; Z_m contact impedance, Z interfacial impedance, R_{el} electrolyte resistance

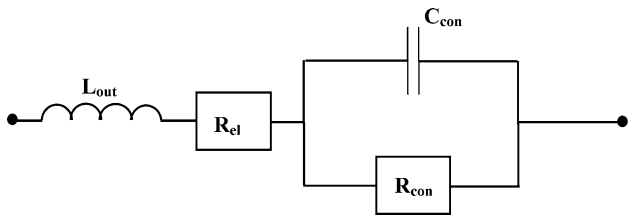

Fig. 9 Equivalent circuit of contact impedance Z_m together with electrolyte resistance R_{el} and L_{out} outer inductance of the system; C_{con} contact capacitance, R_{con} contact resistance

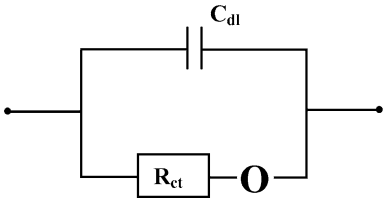

Fig. 10 Equivalent circuit of interfacial impedance Z; C_{dl} double layer capacity, R_{ct} charge transfer resistance, "O" diffusion element which deals with finite thickness of the diffusion layer defined by Eq. 10

particles in the electrolyte (Table 1). (For details see the Appendix).

An important result from the calculation and non-linear regression analysis according to the model of the average dynamic behaviour of a suspension is a decrease in the electrolyte resistivity R_{el}, as a function of specific surface a (Fig. 12), which can be expressed as:

$$a = \frac{A_s}{V_s}(1-\varepsilon) \tag{5}$$

where A_s is the area of the powder particles, V_s is the volume of the particle (solid) phase and ε is a voidage factor defined by Eq. 1. If A_p is the area and V_p is the volume of a single sphere of diameter d_p then

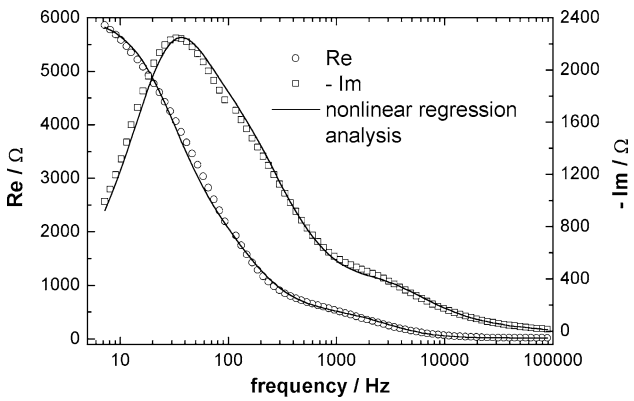

Fig. 11 Impedance diagram of the system consisting of 6 g iron powder 100–125 µm fraction in $NiSO_4$ electrolyte under *dc* polarization of –600 mV versus RE

$$V_s = \sum_i V_{p,i} \tag{6}$$

$$A_s = \sum_i A_{p,i} \tag{7}$$

where $V_p = \frac{\pi}{6} d_p^3$ for a single particle and $A_p = \pi\, d_p^2$. For spherical particles a can be expressed as

$$a = \frac{\sum_i A_{p,i}}{\sum_i V_{p,i}}(1-\varepsilon) = \frac{\sum_i \pi d_{p,i}}{\sum \frac{\pi}{6} d_p^3}(1-\varepsilon) \tag{8}$$

All powder particles in each particle fraction can be regarded as having the same size; thus the specific surface a can be expressed as

$$a = \frac{6}{d_p}(1-\varepsilon) \tag{9}$$

From all three curves in Fig. 12 it can be seen that the increasing number of particles implies a decrease in resistivity of the system. The highest resistivity occurs with the particle fraction 100–125 µm due to the fact that there was no activation of the surface of these particles before experiments were carried out. The slope of the decrease in resistivity is approximately the same for all particle size fractions. The higher resistivity of the smallest particles in comparison with the biggest is due to the hydroxycomplexes of Fe and Ni. The smaller the diameter of the particles the higher the amount of the less-conducting hydroxycomplexes of Ni and Fe accruing in the system [12]. When the conductivity of the electroactive suspension is compared with that of the electroinactive one, a significant difference is observed. In the case of the electroactive suspension a decrease in resistivity is observed, whereas an enhancement in resistivity is observed in the case of the electroinactive one. It can be concluded that the electrochemical reaction occurring on the particle surface plays an important role in the transfer of charge in the heterogeneous system.

As mentioned previously and seen in Fig. 12, active participation of conducting Fe particles in the transfer of charge in the heterogeneous system was observed. Therefore, the contact impedance Z_m (Fig. 8) plays an important role in the total impedance Z_T of the system.

As seen from Table 1, the contact capacitance C_{con}, a part of contact impedance Z_m, is almost independent of the amount of Fe powder added because all mutual contacts between particles have the same nature. In contrast, the contact resistance R_{con}, the second part of Z_m, depends on the weight of added Fe powder

Table 1 Values of the equivalent circuit parameters (Figs. 9 and 10) derived from non-linear regression analysis

Quantity	Fraction 63–100 μm				Fraction 100–125 μm				Fraction 125–160 μm			
	1 g	2 g	6 g	10 g	2 g	4 g	6 g	10 g	1 g	2 g	6 g	10 g
L_{out} / × 10^{-6} H	8.97	9.45	9.33	9.45	10.4	8.69	10.0	10.1	9.05	8.97	8.28	10.6
C_{con} / nF	232	248	210	343	115	106	114	103	113	122	135	88.7
R_{ct} / Ω cm^{-2}	13.7	10.3	1.24	0.067	17.8	4.10	3.90	1.52	115	33.7	2.43	0.422
C_{dl}/μ F m^{-2}	39.0	15.2	9.20	26.9	48.7	27.1	7.46	5.22	519	218	75.6	28.8
Y_0 × 10^6	90.4	63.3	135	264	32.0	31.8	26.4	37.2	112	53.7	271	688
B / $s^{1/2}$	0.109	0.119	0.386	0.092	0.326	0.220	0.111	0.100	0.478	0.320	0.071	0.100

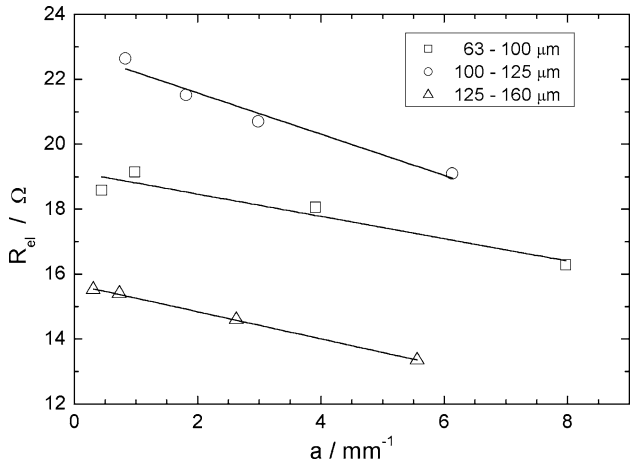

Fig. 12 Electrolyte resistivity of the suspension, R_{el} as a function of specific surface, a for all particle size fractions

(Fig. 13). The anomalous behaviour of the system can be explained by the formation of aggregates or chains of particles with increasing number of powder particles. The more particles present, the higher the probability of forming aggregates or chains [6]. The relative decreases in the contact resistance are presented in Fig. 13.

It is known, that the double-layer surrounding each solid particle plays an important role in charge transfer [15]. Therefore the double-layer capacity gives useful information about charge transfer through the heterogeneous system. In Table 1 a decreasing trend of double-layer capacity with increasing number of Fe particles is observed. This is a sign that with increase in the number of powder particles the ''active'' powder area relatively decreases. The double-layer is formed not only around single particles but also around bigger ''clusters''. This mimics aggregation of particles as mentioned in the case of the contact resistance, R_{con}.

Values of the charge transfer resistance multiplied by the area of the powder particles $R_{ct}*A_s$ does not vary much with particle size or with specific surface a (Fig. 14). The largest values of this product were recorded for 100–125 μm particles because their surface was not activated prior to the experiment. A similar effect

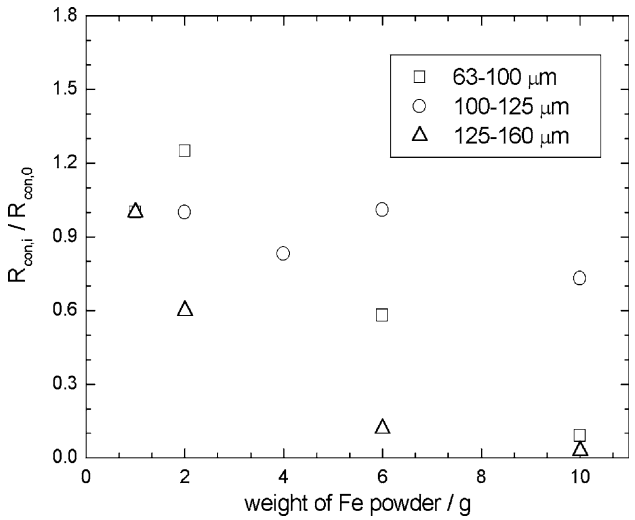

Fig. 13 Relative decrease of the contact resistance $R_{con,i}/R_{con,0}$ as a function of the weight of added iron powder presented in the system; $R_{con,0}$- contact resistance for the lowest particle mass added to the system for each particle fraction

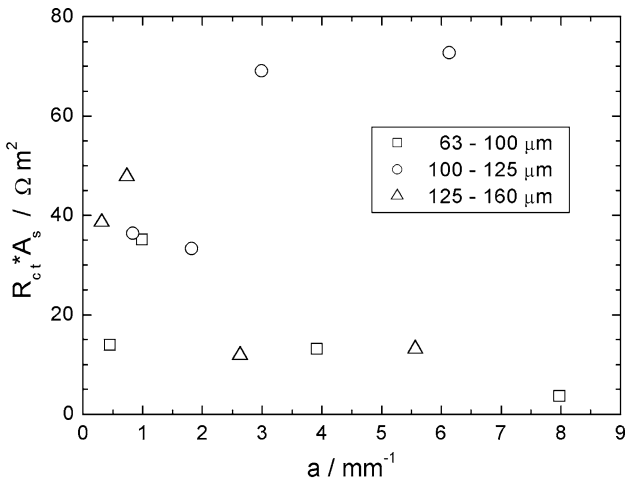

Fig. 14 Charge transfer resistance multiplied by area of particle surface calculated according the model $R_{ct}*A_s$ as a function of specific surface a

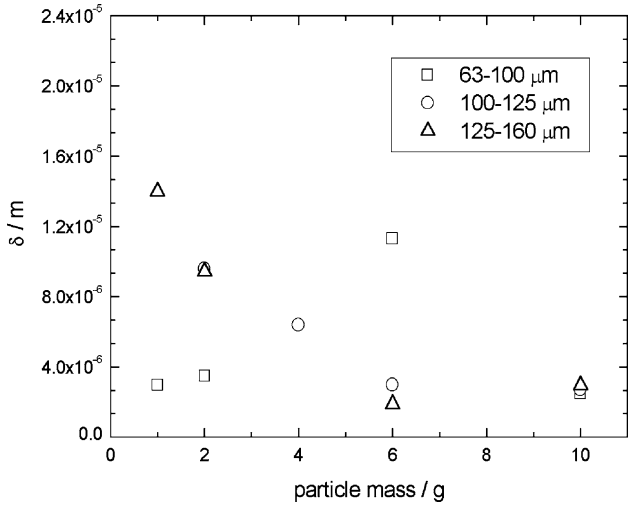

Fig. 15 Thickness of diffusion layer δ as a function of iron particle mass

was observed in the change in resistivity of the stirred system R_{el} (Fig. 12).

Even though the system was stirred the diffusion process cannot be neglected. The two-parameter diffusion element ''O'' must be implemented in the equivalent circuit (Fig. 10). From Table 1, linear dependences of the first parameter Y_0 of the diffusion element ''O'' on m can be seen. The slope of the linear dependence of Y_0 on m is smallest for the middle particle size fraction due to the inactivated surface.

The second parameter B of the diffusion element ''O'' is directly proportional to the thickness of the diffusion layer δ (Eq. 3). The changes in δ with the mass of particles are shown in Fig. 15.

4 Conclusions

The electrochemical behaviour of the stirred heterogeneous system of Fe powder particles-electroactive $NiSO_4$ electrolyte and Fe(pp)-electroinactive Na_2SO_4 electrolyte was represented by conductance measurements and also by EIS. Addition of the powder to the electrolyte causes changes in the appearance of both the conductance and impedance plots. From the conductance data, an inhibition of charge transfer in the Na_2SO_4-Fe suspension is observed. With increase in suspension density this effect is relatively reduced and reaches a limiting value. This is similar to the case of the impedance measurements where there is the evidence of the participation of Fe powder in the charge transfer. The conductivity of the $NiSO_4$-Fe suspension varies with time. At high suspension densities, the particles form aggregates, which also participate in charge transfer. For the evaluation of the equivalent circuits parameters direct calculations and AUTOLAB software developed by Eco Chemie (Holland) were used. The influence of various phenomena governing the dynamic behaviour of the stirred heterogeneous system can be ascertained from the impedance diagrams. On the impedance curve obtained at—600 mV *dc* polarization versus reference electrode, a loop was observed in high-frequency region in both Na_2SO_4 and $NiSO_4$ electrolytes. This new high frequency loop is related to the intermittent contact between particles in the bulk of both electroactive and electroinactive electrolyte. The same behaviour was observed in a fluidized bed [7, 16]. After the addition of Fe powder to the $NiSO_4$ electrolyte the second, low-frequency region loop of the impedance spectrum (below 1 kHz) changed significantly. In the case of Na_2SO_4 electrolyte no second loop in the impedance diagram is seen. Diffusion behaviour can be assigned to the reduction of the dissolved oxygen in Na_2SO_4 electrolyte.

From the impedance diagrams and the proposed model [12] the formation of aggregates and chains of iron particles in the case of high $NiSO_4$(el)-Fe(pp) suspension density is evident. The role of the electrochemical reaction proceeding at the particle surface in charge transfer in heterogeneous stirred systems must also be emphasized.

Acknowledgements The authors express their gratitude to the Grant Agency of the Slovak Republic for financial support of projects 1/ 9038/02 and 1/9425/02.

Appendix

Derivation of the total impedance Z_T of the system according to Figs. 9 and 10

The total impedance of the system is the sum of the electrolyte impedance Z_{el}, contact impedance Z_{con}, interfacial impedance Z as depicted in Fig. 8. Also the outer impedance Z_{out} of the system should be included in the expression for Z_T.

$$Z_T = Z_{out} + Z_{el} + Z_{con} + Z \tag{A.1}$$

For the partial impedances Z_{out}, Z_{el}, Z_{con}, Z according Figs. 9 and 10 it can be written

$$Z_{el} = R_{el} \tag{A.2}$$

$$Z_{out} = i\omega L_{out} \tag{A.3}$$

$$\frac{1}{Z_{con}} = i\omega C_{con} + \frac{1}{R_{con}} \quad \Rightarrow$$
$$Z_{con} = \frac{R_{con}}{(\omega C_{con} R_{con})^2 + 1} - i\frac{\omega C_{con} R_{con}^2}{(\omega C_{con} R_{con})^2 + 1} \quad \text{(A.4)}$$

$$\frac{1}{Z} = \frac{1}{Z_{dl}} + \frac{1}{Z_{ct} + Z_{dif}} \quad \Rightarrow \quad Z = \frac{Z_{dl}(Z_{ct} + Z_{dif})}{Z_{dl} + Z_{ct} + Z_{dif}} \quad \text{(A.5)}$$

where

$$\mathrm{Z_{dl}} = -\frac{\mathrm{i}}{\omega \mathrm{C_{dl}}} \quad \text{(A.6)}$$

$$\mathrm{Z_{ct}} = \mathrm{R_{ct}} \quad \text{(A.7)}$$

$$\mathrm{Z_{dif}} = O = \frac{1}{\mathrm{Y_0}\sqrt{\mathrm{i}\omega}} \tanh\left(\mathrm{B}\sqrt{\mathrm{i}\omega}\right) \quad \text{(A.8)}$$

Z_{dl} is double-layer impedance, Z_{ct} charge transfer impedance and Z_{dif} diffusion impedance.

Applying the Moivre theorem $(\mathrm{a+bi})^{1/\mathrm{n}} = \mathrm{r}^{1/\mathrm{n}}\left(\cos\frac{2\mathrm{l}\pi+\varphi}{\mathrm{n}} + \mathrm{i}\sin\frac{2\mathrm{l}\pi+\varphi}{\mathrm{n}}\right)$
where
$\mathrm{l} = 0, 1, 2 \ldots (\mathrm{n}-1)$; $\mathrm{r} = (\mathrm{a}^2 + \mathrm{b}^2)^{1/2}$; $\tan\varphi = \frac{\mathrm{b}}{\mathrm{a}}$ and if

$$\tanh(\mathrm{x} \pm \mathrm{iy}) = \frac{\sinh(2\mathrm{x}) \pm \sin(2y)}{\cosh(2\mathrm{x}) + \cos(2\mathrm{y})}$$

$\sqrt{\mathrm{i}}$ can be rewritten as $\frac{1+\mathrm{i}}{\sqrt{2}}$ and then

$$\frac{1}{\mathrm{Y_0}\sqrt{\mathrm{i}\omega}} = \frac{\sqrt{2}}{\mathrm{Y_0}\sqrt{\omega}(1\text{-i})} = \sqrt{\frac{2}{\omega}}\frac{1}{2\mathrm{Y_0}} + \mathrm{i}\sqrt{\frac{2}{\omega}}\frac{1}{2\mathrm{Y_0}} \quad \text{(A.9)}$$

$$\tanh\left(\mathrm{i}^{1/2}\mathrm{B}\sqrt{\omega}\right) = \tanh\left((1+\mathrm{i})\mathrm{B}\sqrt{\frac{\omega}{2}}\right) = \frac{\sinh\left(2\mathrm{B}\sqrt{\frac{\omega}{2}}\right) + \mathrm{i}\sin\left(2\mathrm{B}\sqrt{\frac{\omega}{2}}\right)}{\cosh\left(2\mathrm{B}\sqrt{\frac{\omega}{2}}\right) + \cos\left(2\mathrm{B}\sqrt{\frac{\omega}{2}}\right)} \quad \text{(A.10)}$$

After combining Eqs. A.8–A.10 we obtain an expression for Z_{dif}

$$Z_{dif} = \frac{\sqrt{2}[\sinh(2\alpha) - \sin(2\alpha)]}{2Y_0\sqrt{\omega}[\cosh(2\alpha) + \cos(2\alpha)]} + i\frac{\sqrt{2}[\sinh(2\alpha) - \sin(2\alpha)]}{2Y_0\sqrt{\omega}[\cosh(2\alpha) + \cos(2\alpha)]} \quad \text{(A.11)}$$

where $\alpha = \mathrm{B}\sqrt{\frac{\omega}{2}}$.

Then the expression for the total impedance Z_T can be derived as

$$Z_T = i\omega L_{out} + R_{el} + \frac{R_{con}}{i\omega C_{con} R_{con} + 1} + \frac{i\left(R_{ct} + Y_0\sqrt{i\omega} + \tanh\left(B\sqrt{i\omega}\right)\right)}{iY_0\sqrt{i\omega} - R_{ct}C_{dl}Y_0\omega\sqrt{i\omega} - \omega C_{dl}\tanh\left(B\sqrt{i\omega}\right)} \quad \text{(A.12)}$$

$$\mathrm{Z'_T} = \mathrm{R_{el}} + \frac{\mathrm{R_{con}}}{1 + (\omega \mathrm{C_{con}} \mathrm{R_{con}})^2} + \frac{\frac{\sqrt{2}}{2}\frac{(1 + \mathrm{R_{ct}}\sqrt{\omega})(\sinh 2\alpha + \sin 2\alpha)}{\mathrm{R_{ct}}\mathrm{C_{dl}}\mathrm{Y_0}\omega(\cosh 2\alpha + \cos 2\alpha)}}{\left[\mathrm{R_{ct}} + \frac{\sqrt{2}}{2}\frac{\sinh 2\alpha - \sin 2\alpha}{\mathrm{Y_0}\sqrt{\omega}(\cosh 2\alpha + \cos 2\alpha)}\right]^2 + \left[\frac{\sqrt{2}}{2}\frac{\sinh 2\alpha + \sin 2\alpha}{\mathrm{Y_0}\sqrt{\omega}(\cosh 2\alpha + \cos 2\alpha)} - \frac{1}{\omega \mathrm{R_{ct}}}\right]^2} \quad \text{(A.13)}$$

$$\mathrm{Z''_T} = \omega \mathrm{L_{out}} - \frac{\omega \mathrm{C_{con}} \mathrm{R_{con}^2}}{1 + (\omega \mathrm{C_{con}} \mathrm{R_{con}})^2} - \frac{\frac{\sqrt{2}}{2}\frac{\mathrm{Y_0}(\sinh 2\alpha + \sin 2\alpha)\left(2\mathrm{Y_0}\mathrm{R_{ct}^2}\omega - 1\right) + 2\mathrm{R_{ct}}\sqrt{\omega}\left(\sinh^2 2\alpha + \sin^2 2\alpha\right)}{\mathrm{C_{dl}}\mathrm{Y_0^2}\omega^{5/2}\mathrm{R_{ct}}(\cosh 2\alpha + \cos 2\alpha)}}{\left[\mathrm{R_{ct}} + \frac{\sqrt{2}}{2}\frac{\sinh 2\alpha - \sin 2\alpha}{\mathrm{Y_0}\sqrt{\omega}(\cosh 2\alpha + \cos 2\alpha)}\right]^2 + \left[\frac{\sqrt{2}}{2}\frac{\sinh 2\alpha + \sin 2\alpha}{\mathrm{Y_0}\sqrt{\omega}(\cosh 2\alpha + \cos 2\alpha)} - \frac{1}{\omega \mathrm{R_{ct}}}\right]^2} \quad \text{(A.14)}$$

References

1. Sabacky BJ, Evans JW (1977) Metall Trans 8B:5
2. Fleischmann M, Oldfield JW (1971) J Electroanal Chem 29:231
3. Beenackers AA, van Swaaij WP, Welmers A (1977) Electrochim. Acta 22:1277
4. Huh T, Evans JW (1978) J Electrochem Soc 134:308
5. Huh T, Evans JW (1987) J Electrochem Soc 134:317
6. Plimley RE, Wright AR (1984) Chem Eng Sci 39:395
7. Gabrielli C, Huet F, Sarah A and Valentin G (1992) J Appl Electrochem 22: 801
8. Gálová M, OriňákováR, Lux L (1998) J Solid State Electrochem 2:2
9. Gál M, Gálová M, Turoňová A (2000) Collect Czech Chem Commun 65:1515
10. Lux L, Gálová M, Oriňáková R, Turoňová A (1998) Particul Sci Technol 16:135
11. Oriňáková R (2003) Surf Coat Technol 162:54
12. Gál MF (2004) PhD thesis, Slovak University of Technology, Bratislava
13. Roušar I, Micka K, Kimla A (1986) Electrochemical engineering 2. Academia Praha, p 93
14. Pospíšil L, Fiedler J, Fanelli N (2000) Rev Sci Instrum 71:1804
15. Bockris JO'M, Kim J (1997) J Appl Electrochem 27:890
16. Gabrielli C, Huet F, Sarah A, Valentin G (1994) J Appl Electrochem 24:481